frontiers in Pediatrics

ORIGINAL RESEARCH
published: 15 January 2021
doi: 10.3389/fped.2020.617548

Changes of Structural Brain Network Following Repetitive Transcranial Magnetic Stimulation in Children With Bilateral Spastic Cerebral Palsy: A Diffusion Tensor Imaging Study

Wenxin Zhang[1†], *Shang Zhang*[1†], *Min Zhu*[1], *Jian Tang*[1], *Xiaoke Zhao*[1], *Ying Wang*[2], *Yuting Liu*[2], *Ling Zhang*[1*] and *Hong Xu*[1*]

[1] Department of Rehabilitation, Children's Hospital of Nanjing Medical University, Nanjing, China, [2] Department of Radiology, Children's Hospital of Nanjing Medical University, Nanjing, China

OPEN ACCESS

Edited by:
Marco Carotenuto,
University of Campania Luigi Vanvitelli, Italy

Reviewed by:
Daniela Smirni,
University of Palermo, Italy
Michele Roccella,
University of Palermo, Italy

***Correspondence:**
Ling Zhang
hdyxyzl@126.com
Hong Xu
xuhong198616@163.com

[†]These authors share first authorship

Specialty section:
This article was submitted to Pediatric Neurology, a section of the journal Frontiers in Pediatrics

Received: 06 November 2020
Accepted: 09 December 2020
Published: 15 January 2021

Citation:
Zhang W, Zhang S, Zhu M, Tang J, Zhao X, Wang Y, Liu Y, Zhang L and Xu H (2021) Changes of Structural Brain Network Following Repetitive Transcranial Magnetic Stimulation in Children With Bilateral Spastic Cerebral Palsy: A Diffusion Tensor Imaging Study. Front. Pediatr. 8:617548. doi: 10.3389/fped.2020.617548

Introduction: Bilateral spastic cerebral palsy (BSCP) is the most common subtype of cerebral palsy (CP), which is characterized by various motor and cognitive impairments, as well as emotional instability. However, the neural basis of these problems and how repetitive transcranial magnetic stimulation (rTMS) can make potential impacts on the disrupted structural brain network in BSCP remain unclear. This study was aimed to explore the topological characteristics of the structural brain network in BSCP following the treatment of rTMS.

Methods: Fourteen children with BSCP underwent 4 weeks of TMS and 15 matched healthy children (HC) were enrolled. Diffusion tensor imaging (DTI) data were acquired from children with bilateral spastic cerebral palsy before treatment (CP1), children with bilateral spastic cerebral palsy following treatment (CP2) and HC. The graph theory analysis was applied to construct the structural brain network. Then nodal clustering coefficient (C_i) and shortest path length (L_i) were measured and compared among groups.

Results: Brain regions with significant group differences in C_i were located in the left precental gyrus, middle frontal gyrus, calcarine fissure, cuneus, lingual gyrus, postcentral gyrus, inferior parietal gyri, angular gyrus, precuneus, paracentral lobule and the right inferior frontal gyrus (triangular part), insula, posterior cingulate gyrus, precuneus, paracentral lobule, pallidum. In addition, significant differences were detected in the L_i of the left precental gyrus, lingual gyrus, superior occipital gyrus, middle occipital gyrus, superior parietal gyrus, precuneus and the right median cingulate gyrus, posterior cingulate gyrus, hippocampus, putamen, thalamus. *Post hoc t*-test revealed that the CP2 group exhibited increased C_i in the right inferior frontal gyrus, pallidum and decreased L_i in the right putamen, thalamus when compared with the CP1 group.

Conclusion: Significant differences of node-level metrics were found in various brain regions of BSCP, which indicated a disruption in structural brain connectivity in BSCP.

The alterations of the structural brain network provided a basis for understanding of the pathophysiological mechanisms of motor and cognitive impairments in BSCP. Moreover, the right inferior frontal gyrus, putamen, thalamus could potentially be biomarkers for predicting the efficacy of TMS.

Keywords: cerebral palsy, diffusion tensor imaging, structural brain network, graph theory, repetitive transcranial magnetic stimulation

INTRODUCTION

Cerebral palsy (CP) is considered as an early childhood-onset neurodevelopmental disorder, which is characterized by motor and postural dysfunction often accompanied by cognitive impairments (1, 2). Bilateral spastic cerebral palsy (BSCP) is one of the most common CP subtype, which can also lead to cognitive disabilities and learning disabilities (3, 4). Repetitive transcranial magnetic stimulation (rTMS) is a non-invasive neuromodulation technique, which has been widely used for rehabilitation of CP (5, 6). In addition, the emerging magnetic resonance imaging (MRI) technique, especially diffusion tensor imaging (DTI), provides a non-invasive tool to explore white matter changes of CP and has recently advance our current understanding of the pathogenesis of CP (7–9). Therefore, there is a need to explore the effect of rTMS in the treatment of CP and identify changes of the brain networks that were modulated by the rTMS intervention.

DTI is a sensitive method to detect the microstructure of white matter, which allows the reconstruction of neuronal pathways (10–12). Previous DTI studies identified moderate and severe white matter abnormalities in the brain of CP, which could predict the neurocognitive and behavioral impairments of patients (13, 14). Children with spastic CP were found to be associated with the corticospinal tract lesions, which might lead to the motor impairments and help the early and highly accuracy diagnosis of spastic CP (14–16). In addition, the abnormal structure of basal ganglia and thalamus were found in CP children by the method of MRI, which were considered to be related to the motor and postural dysfunction of CP (17, 18). However, the abnormalities of a single white matter tract or an independent brain region could not able to reflect the pathophysiological mechanisms of motor and cognitive dysfunction in CP. Widespread abnormalities were found in the cerebral cortex and subcortical structures of CP children.

Graph theory provides a powerful mathematical framework and some metrics, which can describe the topological features of the brain networks. The brain network consisted of nodes (brain areas) and edges (structural connections between brain areas) can reflected the connectivity of all regions in the brain. Previous DTI-based brain network study showed that CP children had aberrant nodal parameters in the sensorimotor cortex (19). Distributed network-level structural disruptions and widespread changed topological characteristics of local brain regions might be associated with the pathogenesis of neurosensory and cognitive impairments of CP, such as the posterior-anterior neural network (20, 21). Moreover, abnormal nodal parameters were found in the prefrontal cortex, motor areas, cingulate gyrus and occipital cortex of CP, which might contribute to the motor dysfunction of patients, as well as cognitive impairments (19). Moreover, substantial functional reorganization of the motor cortex and corticospinal projections were found in CP children after the treatment of rTMS, which demonstrated that it was a possible treatment for neurodevelopmental disorders (6). However, little is known about how the rTMS modulates the topological characteristics of the structural brain network in BSCP children.

The present study was aimed to perform a DTI based investigation of topological characteristics of the structural brain network in BSCP following the treatment of rTMS. Based on the findings of previous studies, we hypothesized that BSCP children might had improved motor function, as well as changes of structural brain connectivity after the treatment of rTMS.

MATERIALS AND METHODS

Participants

A total of 14 children with BSCP were recruited from the department of rehabilitation in Children's Hospital of Nanjing Medical University. The clinical features and MRI scanning of participants were used for the diagnosis of BSCP through standardized assessment by two neurologists. Fifteen healthy children (HC) age- and sex-matched without neurological and psychiatric disorders were recruited. In addition, the Gross Motor Function Classification System (GMFCS) (22) and Gesell Developmental Schedules (Gesell) (23) were conducted to assess the level of motor and cognitive function of all participants including patients before and following the treatment of rTMS.

The inclusion criteria were as follows: (1) diagnosis of BSCP according to strict criteria; (2) right-handed; (3) age$\leq$24 months; (4) no history of trauma or brain operation;

TABLE 1 | Demographic and clinical characteristics.

Characteristics	CP1 ($N = 14$)	CP2 ($N = 14$)	HC ($N = 16$)	P
Age (months, mean ± SD)	16.64 ± 4.70	16.64 ± 4.70	15.47 ± 4.26	0.72
Gender (N)	9 M/5 F	9 M/5 F	8 M/7 F	0.78
Gesell (mean ± SD)	59.50 ± 8.11	67.79 ± 9.00	96.20 ± 5.91	0.00
GMFCS (N)	II: 4; III: 7; IV: 3	II: 9; III: 5	–	–

CP1, children with bilateral spastic cerebral palsy before treatment; CP2, children with bilateral spastic cerebral palsy following treatment; HC, health children. N, number of participants; M, male, F, female; SD, standard deviation; Gesell, Gesell Developmental Schedules; GMFCS, Gross Motor Function Classification System; Gender was analyzed using chi-square test; Age, the scores of Gesell was analyzed using one-way analysis of variance. $P < 0.05$ indicated statistically significant differences.

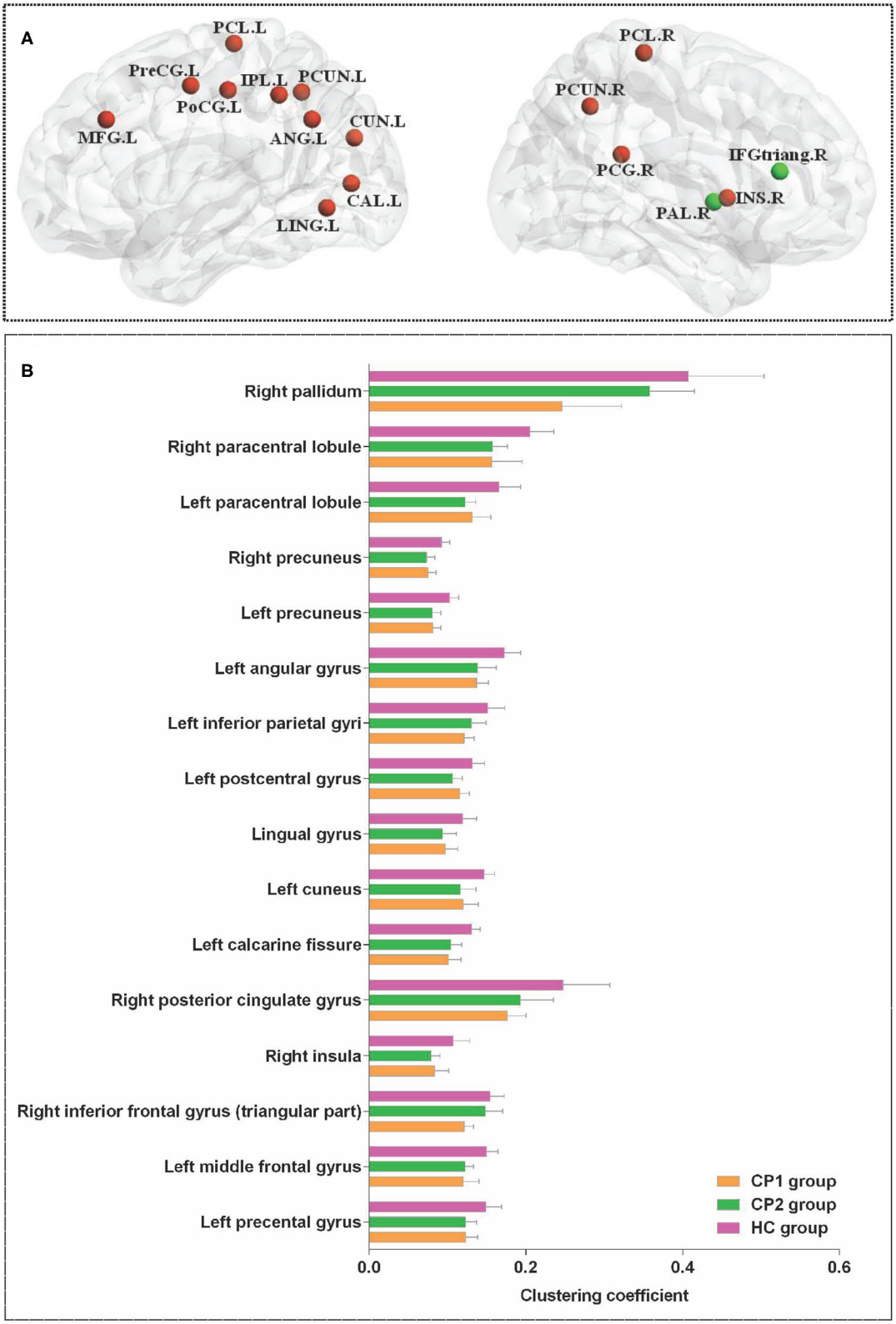

FIGURE 1 | Brain regions with significant group effects in the nodal clustering coefficient among the three groups (ANOVA; FDR-corrected $P < 0.05$). CP1, children with bilateral spastic cerebral palsy before treatment; CP2,children with bilateral spastic cerebral palsy following treatment; HC, health children. **(A)** Brain regions with significant group differences; **(B)** statistical comparisons among the three groups. ANOVA: one-way analysis of variance. FDR: false discovery rate. FDR-corrected $P < 0.05$ indicated statistically significant differences among the three groups.

TABLE 2 | Brain regions with significant group effects in the nodal clustering coefficient among the three groups (ANOVA; FDR-corrected $P<0.05$).

Brain regions	Nodal clustering coefficient			*F*	*P*
	CP1	CP2	HC		
Left precental gyrus	0.12 ± 0.016	0.12 ± 0.015	0.15 ± 0.020	11.07	0.00015
Left middle frontal gyrus	0.12 ± 0.020	0.12 ± 0.011	0.15 ± 0.015	16.04	0.000008
Right inferior frontal gyrus (triangular part)	0.12 ± 0.012	0.15 ± 0.023	0.15 ± 0.018	13.17	0.00004
Right insula	0.08 ± 0.018	0.08 ± 0.011	0.11 ± 0.021	10.60	0.0002
Right posterior cingulate gyrus	0.18 ± 0.024	0.19 ± 0.042	0.25 ± 0.060	9.76	0.000354
Left calcarine fissure	0.10 ± 0.016	0.10 ± 0.014	0.13 ± 0.011	20.23	0.000001
Left cuneus	0.12 ± 0.020	0.12 ± 0.020	0.15 ± 0.014	12.24	0.000071
Left lingual gyrus	0.10 ± 0.016	0.09 ± 0.018	0.12 ± 0.018	10.08	0.00029
Left postcentral gyrus	0.12 ± 0.012	0.11 ± 0.013	0.13 ± 0.016	12.00	0.000083
Left inferior parietal gyri	0.12 ± 0.013	0.13 ± 0.019	0.15 ± 0.022	10.58	0.00021
Left angular gyrus	0.14 ± 0.015	0.14 ± 0.024	0.17 ± 0.021	14.64	0.000017
Left precuneus	0.08 ± 0.010	0.08 ± 0.011	0.10 ± 0.012	18.83	0.000002
Right precuneus	0.07 ± 0.011	0.07 ± 0.011	0.09 ± 0.010	14.79	0.000016
Left paracentral lobule	0.13 ± 0.024	0.12 ± 0.014	0.17 ± 0.028	14.50	0.000018
Right paracentral lobule	0.16 ± 0.039	0.16 ± 0.020	0.21 ± 0.030	12.24	0.000071
Right pallidum	0.25 ± 0.076	0.36 ± 0.057	0.41 ± 0.096	15.86	0.000008

CP1, children with bilateral spastic cerebral palsy before treatment; CP2, children with bilateral spastic cerebral palsy following treatment; HC, health children. ANOVA: one-way analysis of variance. FDR, false discovery rate. FDR-corrected $P < 0.05$ indicated statistically significant differences among the three groups.

(5) no abnormal neuroimaging findings by conventional MRI. The exclusion criteria were as follows: (1) congenital developmental malformations; (2) genetic metabolic diseases; (3) history of nervous system infection; (4) psychiatric disorders; (5) disorders hearing abnormalities; (6) severe visual difficulties.

This study was approved by the Ethics Committee of the Children's Hospital of Nanjing Medical University. The consents were obtained from a parent or guardian on behalf of the participants.

Repetitive Transcranial Magnetic Stimulation

All children received 10 rTMS sessions daily for 2 weeks with a 70-mm figure-of-eight coil magnetic stimulator (YIRUIDE, Wuhan, China) (24). The human cerebral cortex was a complex system with tightly interconnected excitatory and inhibitory neuronal networks. High-frequency (HF) (>5-Hz) rTMS increased cortical excitability, whereas low-frequency (LF) (<1-Hz) rTMS decreased cortical excitability. In addition, high frequency stimulation could enhance cortical excitability, which resulted in improvement in motor function. Low frequency stimulation had an inhibitory effect on the brain function, which decreased motor function. Therefore, the stimulation targeted site was located at left dorsolateral prefrontal cortex (lDLPFC), which was considered to play an important role in the regulation of motor and cognitive function (25, 26). The parameters of rTMS treatment were set based on previous study (27), which demonstrated that the treatment of 10-Hz rTMS could improve the motor and cognitive function of patients. The parameters of rTMS were as follows: 10 Hz, 3 s stimulation, 27 s interval, 110% intensity of resting motor threshold (rMT), 900 pulses per session, a total of 15 min/session.

MRI Data Acquisition

The MRI data of the CP1, CP2 and HC groups were obtained using a 3.0 Tesla Philips MRI scanner at the department of radiology of Children's Hospital of Nanjing Medical University, Nanjing, China. The scan parameters of 3D T1-weighted imaging were as follows: repetition time (TR) = 7.9 ms, echo time (TE) = 3.5 ms, slice thickness = 1 mm, field of view (FOV) = 200 × 200 mm^2, matrix size = 200 × 200, flip angle (FA) = 7.8°. The scan parameters of DTI imaging were as follows: TE = 96 ms, TR = 4,596 ms, slice thickness = 2 mm, FOV = 200 × 200 mm^2, matrix size = 100 × 98, FA = 90°.

MRI Data Preprocessing

The MRI data were preprocessed with the diffusion toolbox of Functional MRI of the Brain (FMRIB) software Library (FSL) (28). Firstly, eddy current and motion artifact correction of the DTI data were performed. Secondly, estimation of the diffusion tensor was performed. Finally, the fractional anisotropy (FA) of each voxel was calculated and then diffusion tensor tractography was performed. Diffusion tensor tractography was implemented using the Diffusion toolkit (http://trackvis.org/dtk/) by the fiber assignment by continuous tracking (FACT) algorithm. The tracts were computed by seeding each voxel with an FA > 0.2. The tractography was terminated if it reached a voxel with an FA < 0.2 or turned an angle >50°.

Brain Network Construction

To define the nodes of the structural brain network, the whole brain were segmented by the automated anatomical

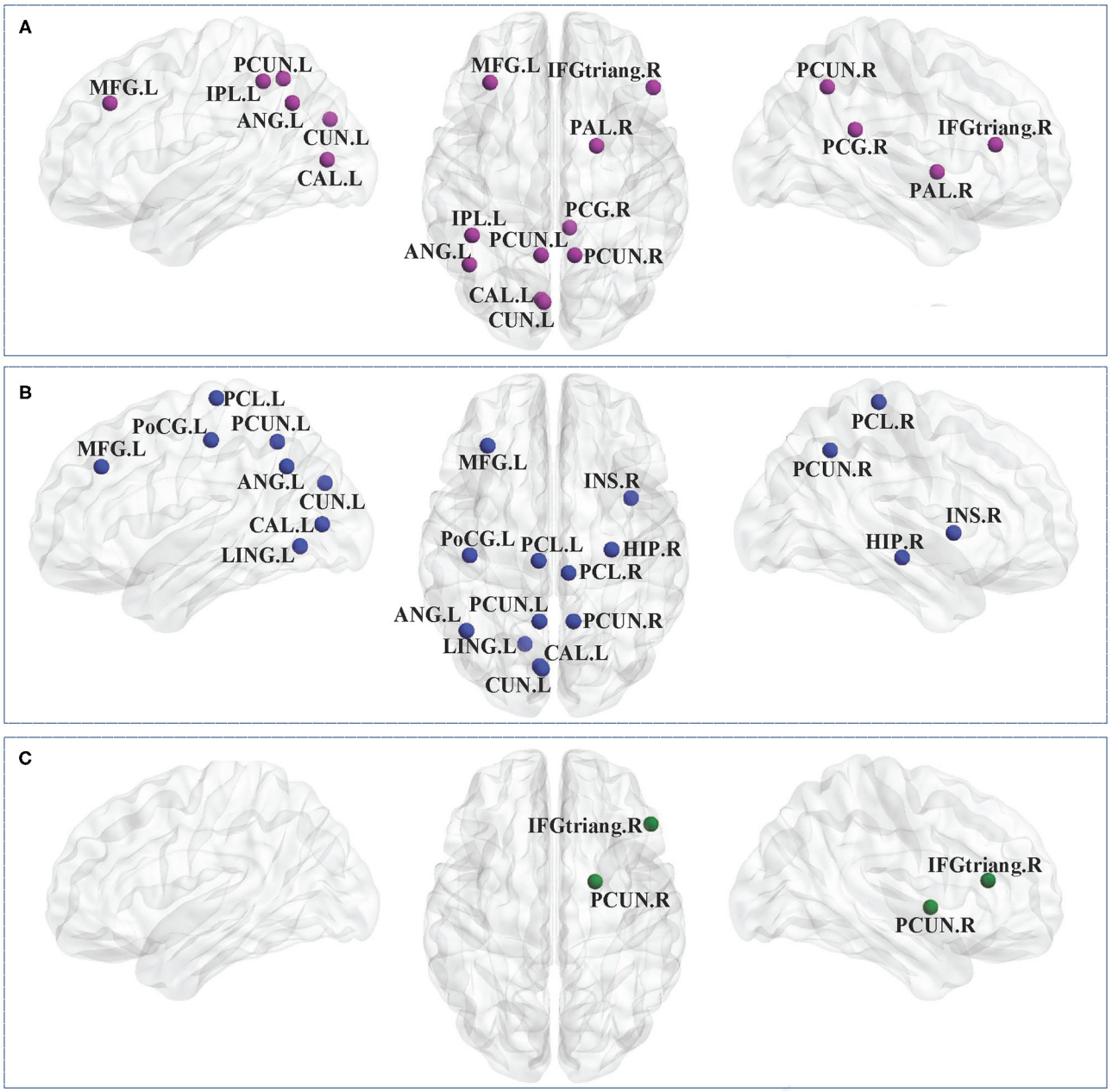

FIGURE 2 | Brain regions with significant group effects in the nodal clustering coefficient between the CP1, CP2, and HC groups (*post hoc t*-test; FDR-corrected $P < 0.05$). CP1, children with bilateral spastic cerebral palsy before treatment; CP2, children with bilateral spastic cerebral palsy following treatment; HC, health children. **(A)** Statistical comparisons between CP1 and HC; **(B)** statistical comparisons between CP2 and HC; **(C)** statistical comparisons between CP1 and CP2. FDR, false discovery rate. FDR-corrected $P < 0.05$ indicated statistically significant differences between groups.

labeling template (AAL) template (29). Then 90 cortical and subcortical regions (45 for each hemisphere) were obtained, which represented the nodes of the brain network. To define the edges between nodes of the brain network, a threshold was selected for the fiber bundles. Two regions were considered structurally connected if there were at least 3 fibers and two endpoints were located in these two regions. Using this procedure, the edges of the brain network were also obtained.

Nodal Characteristics Analysis

Graph theory was used to quantify the nodal characteristics of the structural brain network, which included the nodal clustering coefficient and shortest path length (30). The clustering coefficient of the node (C_i) is defined as the likelihood that the node's neighborhoods are connected with each other, which is often used to investigate the segregation of the node in the network. The shortest path length between nodes is defined as

TABLE 3 | Brain regions with significant group effects in the nodal clustering coefficient between the CP1, CP2, and HC groups (*post hoc t*-test; FDR-corrected $P < 0.05$).

	Brain regions	Nodal clustering coefficient		*t*	*P*
CP1<HC	Left middle frontal gyrus	0.12 ± 0.020	0.15 ± 0.015	−4.50	0.00012
	Right inferior frontal gyrus (triangular part)	0.12 ± 0.012	0.15 ± 0.018	−5.62	0.000006
	Right posterior cingulate gyrus	0.18 ± 0.024	0.25 ± 0.060	−4.07	0.00037
	Left calcarine fissure	0.10 ± 0.016	0.13 ± 0.011	−5.73	0.000004
	Left cuneus	0.12 ± 0.020	0.15 ± 0.014	−4.26	0.00022
	Left inferior parietal gyri	0.12 ± 0.013	0.15 ± 0.022	−4.52	0.00011
	Left angular gyrus	0.14 ± 0.015	0.17 ± 0.021	−5.24	0.000016
	Left precuneus	0.08 ± 0.010	0.10 ± 0.012	−5.13	0.000022
	Right precuneus	0.07 ± 0.011	0.09 ± 0.010	−4.47	0.00013
	Right pallidum	0.25 ± 0.076	0.41 ± 0.096	−4.99	0.000032
CP2<HC	Left middle frontal gyrus	0.12 ± 0.011	0.15 ± 0.015	−5.58	0.000006
	Right insula	0.08 ± 0.011	0.11 ± 0.021	−4.29	0.0002
	Right hippocampus	0.10 ± 0.016	0.13 ± 0.021	−4.18	0.00027
	Left calcarine fissure	0.10 ± 0.014	0.13 ± 0.011	−5.70	0.000005
	Left cuneus	0.12 ± 0.020	0.15 ± 0.014	−4.73	0.000064
	Left lingual gyrus	0.09 ± 0.018	0.12 ± 0.018	−4.02	0.00042
	Left postcentral gyrus	0.11 ± 0.013	0.13 ± 0.016	−4.61	0.000086
	Left angular gyrus	0.14 ± 0.024	0.17 ± 0.021	−4.14	0.00031
	Left precuneus	0.08 ± 0.011	0.10 ± 0.012	−5.21	0.000017
	Right precuneus	0.07 ± 0.011	0.09 ± 0.010	−4.89	0.000041
	Left paracentral lobule	0.12 ± 0.014	0.17 ± 0.028	−5.21	0.000017
	Right paracentral lobule	0.16 ± 0.020	0.21 ± 0.030	−5.03	0.000028
CP1< CP2	Right inferior frontal gyrus (triangular part)	0.25 ± 0.076	0.36 ± 0.057	−3.96	0.00052
	Right pallidum	0.12 ± 0.012	0.15 ± 0.023	−4.39	0.00017

CP1, children with bilateral spastic cerebral palsy before treatment; CP2, children with bilateral spastic cerebral palsy following treatment; HC, health children. FDR-corrected P < 0.05 indicated statistically significant differences between groups.

the length of the path with the shortest length between nodes. The shortest path length of the node (L_i) is defined as the mean of shortest path length between the node i and all other nodes, which is often used to investigate the integration of the node in the network. Therefore, $C_i$indicates the extent of the local interconnectivity of the node i and quantifies the local efficiency of information transfer of the node i (the local efficiency) while L_i quantifies the ability of the node i to propagate information in parallel (the global efficiency).

Statistical Analysis

Two sample t-test was applied to compare the demographic and clinical data between groups. One-way analysis of variance (ANOVA) was performed to compare the values of C_i and L_i among three groups. Then *post hoc* t-test was applied to identify the differences of C_i and L_i between groups. A false discovery rate (FDR) procedure was applied to address the problem of multiple comparisons at a q value of 0.05. The significant level was set at $P < 0.05$ for all statistical tests.

RESULTS

Demographic and Clinical Characteristics

The clinical information of the CP1, CP2 and HC groups were presented in **Table 1**. There were no significant differences in gender ($P = 0.72$) and age ($P = 0.78$) between groups. The CP1 group had lower total scores of Gesell when compared with the groups of CP1 and HC ($P < 0.00$) groups.

Differences of Nodal Clustering Coefficient

Figure 1 showed the brain regions with significant group differences in C_i (ANOVA; FDR-corrected $P < 0.05$). These regions were located in the left precental gyrus, middle frontal gyrus, calcarine fissure, cuneus, lingual gyrus, postcentral gyrus, inferior parietal gyri, angular gyrus, precuneus, paracentral lobule and the right inferior frontal gyrus (triangular part), insula, posterior cingulate gyrus, precuneus, paracentral lobule, pallidum (**Table 2**).

Nodal Clustering Coefficient in CP1 vs. HC

Between-group comparisons revealed that the CP1 group had a significantly decreased C_i in the left middle frontal gyrus, calcarine fissure, cuneus, inferior parietal gyrus, angular gyrus, precuneus and the right inferior frontal gyrus (triangular part), posterior cingulate gyrus, precuneus, pallidum when compared with the HC group (*post hoc* t-test; FDR-corrected $P < 0.05$; **Figure 2** and **Table 3**).

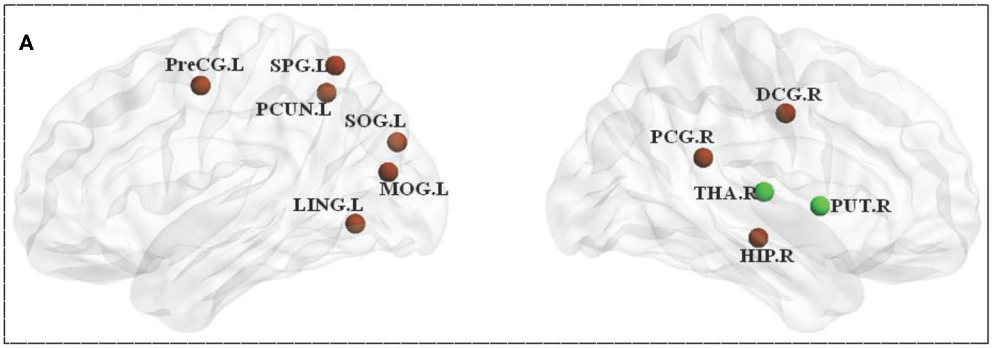

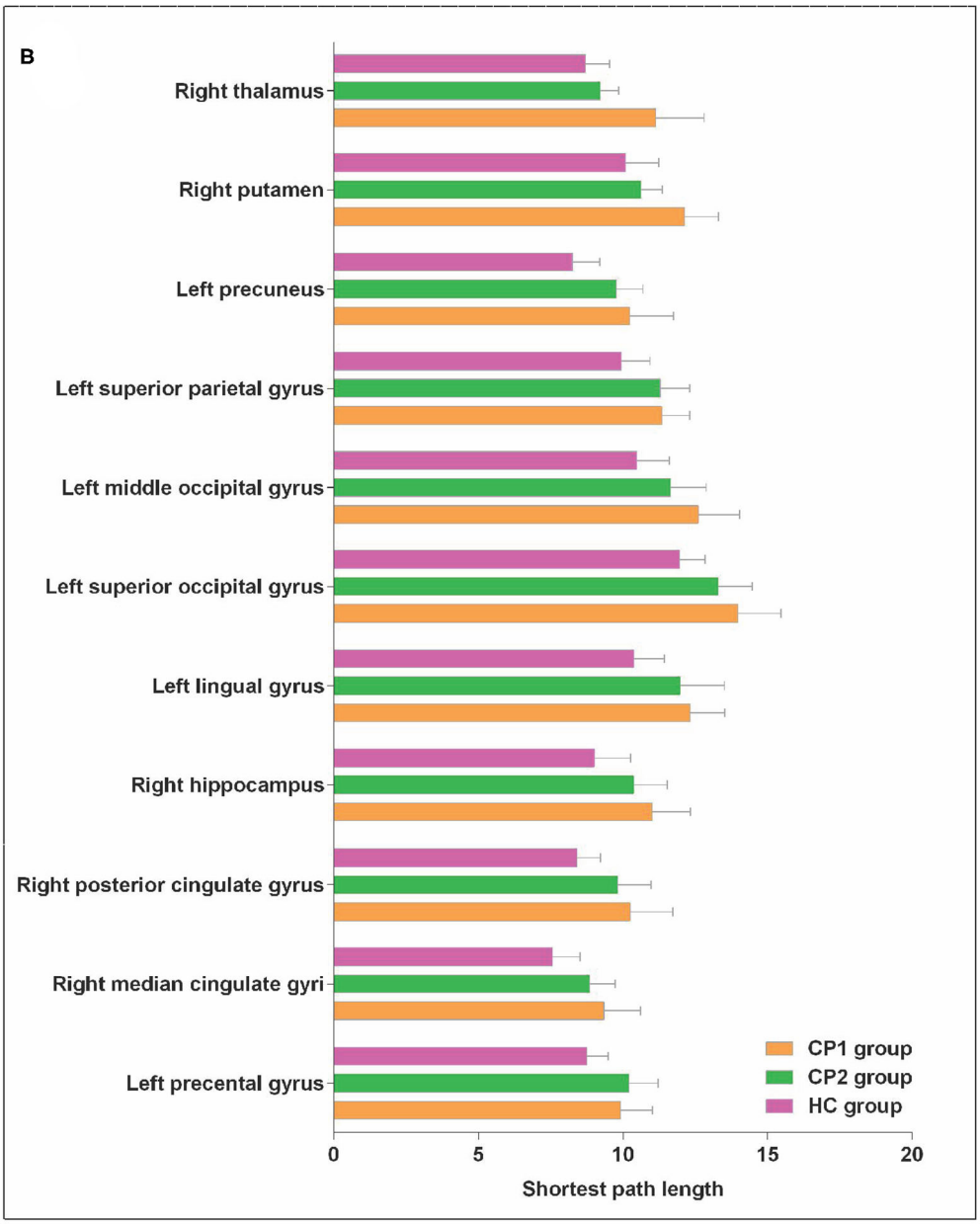

FIGURE 3 | Brain regions with significant group effects in the nodal path length among the three groups (ANOVA; FDR-corrected $P < 0.05$). CP1, children with bilateral spastic cerebral palsy before treatment; CP2, children with bilateral spastic cerebral palsy following treatment; HC, health children. **(A)** Brain regions with significant group differences; **(B)** statistical comparisons among the three groups. ANOVA: one-way analysis of variance. FDR, false discovery rate. FDR-corrected $P < 0.05$ indicated statistically significant differences among the three groups.

TABLE 4 | Brain regions with significant group effects in the nodal path length among the three groups (ANOVA; FDR-corrected $P < 0.05$).

Brain regions	Nodal path length			*F*	*P*
	CP1	CP2	HC		
Left precental gyrus	9.90 ± 1.12	10.21 ± 1.02	8.76 ± 0.72	9.13	0.00054
Right median cingulate gyri	9.34 ± 1.27	8.84 ± 0.89	7.56 ± 0.95	11.29	0.00013
Right posterior cingulate gyrus	10.25 ± 1.47	9.81 ± 1.17	8.41 ± 0.81	9.75	0.00036
Right hippocampus	11.01 ± 1.33	10.37 ± 1.18	9.02 ± 1.24	9.68	0.00037
Left lingual gyrus	12.33 ± 1.20	11.98 ± 1.53	10.36 ± 1.05	9.94	0.00031
Left superior occipital gyrus	13.98 ± 1.49	13.29 ± 1.19	11.96 ± 0.89	10.60	0.0002
Left middle occipital gyrus	12.60 ± 1.43	11.64 ± 1.23	10.47 ± 1.14	10.30	0.00025
Left superior parietal gyrus	11.35 ± 0.97	11.29 ± 1.03	9.94 ± 0.99	9.43	0.00044
Left precuneus	10.23 ± 1.51	9.77 ± 0.91	8.25 ± 0.95	11.85	0.000091
Right putamen	12.12 ± 1.18	10.61 ± 0.75	10.09 ± 1.16	14.55	0.000018
Right thalamus	11.13 ± 1.68	9.21 ± 0.65	8.69 ± 0.84	18.08	0.000003

CP1, children with bilateral spastic cerebral palsy before treatment; CP2, children with bilateral spastic cerebral palsy following treatment; HC, health children. ANOVA: one-way analysis of variance. FDR, false discovery rate. FDR-corrected P < 0.05 indicated statistically significant differences among the three groups.

Nodal Clustering Coefficient in CP2 vs. HC

As shown in **Figure 2** and **Table 3** (*post hoc t*-test; FDR-corrected $P < 0.05$), the CP2 group demonstrated decreased C_i in the left middle frontal gyrus, calcarine fissure, cuneus, lingual gyrus, postcentral gyrus, angular gyrus, precuneus and the right insula, hippocampus, precuneus, paracentral lobule when compared with the HC group.

Nodal Clustering Coefficient in CP2 vs. CP1

Compared with the CP1 group, the CP2 group exhibited increased C_i in the right inferior frontal gyrus and pallidum (*post hoc t*-test; FDR-corrected $P < 0.05$; **Figure 2** and **Table 3**).

Differences of Nodal Path Length

Significant differences were detected among the three groups in the L_i of the left precental gyrus, lingual gyrus, superior occipital gyrus, middle occipital gyrus, superior parietal gyrus, precuneus and the right median cingulate gyrus, posterior cingulate gyrus, hippocampus, putamen, thalamus (ANOVA; FDR-corrected $P < 0.05$; **Figure 3** and **Table 4**).

Nodal Path Length in CP1 vs. HC

The results showed that the CP1 group exhibited significantly increased L_i in the lingual gyrus, superior occipital gyrus, middle occipital gyrus, fusiform gyrus, angular gyrus, precuneus and the right median cingulated gyrus, posterior cingulate gyrus, hippocampus, putamen, thalamus when compared with the HC group (*post hoc t*-test; FDR-corrected $P < 0.05$; **Figure 4** and **Table 5**).

Nodal Path Length in CP2 vs. HC

Figure 4 and **Table 5** showed that the CP2 group had a significantly increased L_i in the left precental gyrus, inferior frontal gyrus (opercular part), postcentral gyrus, precuneus, paracentral lobule and the right supplementary motor area, paracentral lobule when compared with the HC group (*post hoc t*-test; FDR-corrected $P < 0.05$).

Nodal Path Length in CP2 vs. CP1

Post hoc t-test revealed that the CP2 group had decreased L_i in the right putamen and thalamus when compared with the CP1 group (*post hoc t*-test; FDR-corrected $P < 0.05$; **Figure 4** and **Table 5**).

DISCUSSION

Using DTI data and the graph theoretical analysis, we investigated the underlying neural changes following the treatment of rTMS in children with BSCP. The results showed significant differences of node-level metrics in various brain regions, which indicated a disruption in structural brain connectivity in BSCP. Children with BSCP showed significant differences of C_i and L_i in widespread brain areas including the cortical and subcortical regions when compared with HC. In addition, increased C_i of the right inferior frontal gyrus, pallidum and decreased L_i of the right putamen, thalamus were found in the BSCP children following the treatment of rTMS when compared with those of patients before treatment. These findings extended our understanding of the neurophysiologic mechanisms involved in BSCP and the effect of rTMS on changes in structural brain connectivity of BSCP from a network perspective.

Previous neuroimaging studies found that CP children were often associated with diffuse periventricular leukomalacia, which was a high risk factor for CP (31–33). In addition, it had been shown that structural alterations in CP children were not confined to a periventricular leukomalacia or sensorimotor-related brain regions, but were rather widespread across the whole brain of children (34–37). Consistent with the results of previous studies in children with CP (38–40), our results of ANOVA showed that BSCP children had topological alterations of extensive areas in the structural brain networks, which were primarily located in the prefrontal, parietal and occipital cortex, as well as some subcortical regions. The decreased C_i and increased L_i suggested that BSCP children lower structural

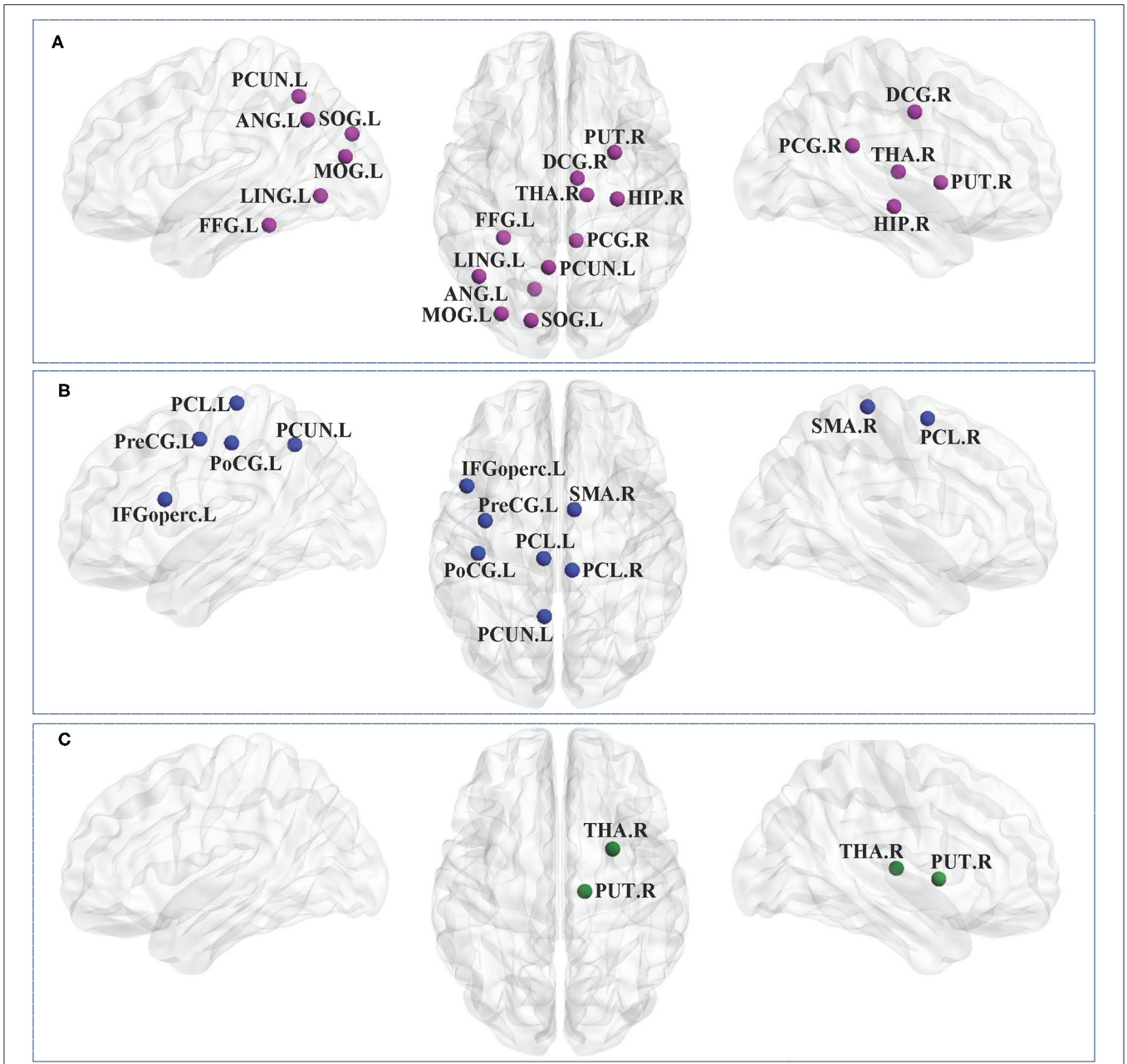

FIGURE 4 | Brain regions with significant group effects in the nodal path length between the CP1, CP2, and HC groups (*post hoc t*-test; FDR-corrected $P < 0.05$). CP1, children with bilateral spastic cerebral palsy before treatment; CP2, children with bilateral spastic cerebral palsy following treatment; HC, health children. **(A)** Statistical comparisons between CP1 and HC; **(B)** statistical comparisons between CP2 and HC; **(C)** statistical comparisons between CP1 and CP2. FDR, false discovery rate. FDR-corrected $P < 0.05$ indicated statistically significant differences between groups.

connections between these regions and other brain regions than HC across the whole brain. These impaired topological architecture implied that the brain network of BSCP children had inefficient information exchange than HC.

Our results also confirmed the clinical therapeutic effect of rTMS on motor and cognition recovery in children with BSCP, which were consistent with the findings of previous studies. It had been identified that the treatment of rTMS could modulate the neuroplasticity below the magnetic coil, as well as the remote cortical and subcortical regions through structural connectivity (41). Children with BSCP in this study showed rTMS-induced changes of the topological characteristics of the structural brain networks. Increased C_i of the right inferior frontal gyrus, pallidum were found in BSCP children following the treatment of rTMS, as well as decreased L_i of the right putamen, thalamus. These results suggested that rTMS could modulate structural

TABLE 5 | Brain regions with significant group effects in the nodal path length between the CP1, CP2, and HC groups (*post hoc t*-test; FDR-corrected $P < 0.05$).

Brain regions	Nodal clustering coefficient		*t*	*P*	
CP1>HC	Right median cingulate gyri	9.34 ± 1.27	7.56 ± 0.95	4.31	0.0002
	Right posterior cingulate gyrus	10.25 ± 1.47	8.41 ± 0.81	4.20	0.00026
	Right hippocampus	11.01 ± 1.33	9.02 ± 1.24	4.19	0.00027
	Left lingual gyrus	12.33 ± 1.20	10.36 ± 1.05	4.68	0.000071
	Left superior occipital gyrus	13.98 ± 1.49	11.96 ± 0.89	4.48	0.00012
	Left middle occipital gyrus	12.60 ± 1.43	10.47 ± 1.14	4.46	0.00013
	Left fusiform gyrus	13.91 ± 1.80	11.82 ± 0.94	3.94	0.00051
	Left angular gyrus	14.64 ± 1.89	11.92 ± 1.69	4.09	0.00035
	Left precuneus	10.23 ± 1.51	8.25 ± 0.95	4.26	0.00022
	Right putamen	12.12 ± 1.18	10.09 ± 1.16	4.70	0.000069
	Right thalamus	11.13 ± 1.68	8.69 ± 0.84	4.99	0.000031
CP2>HC	Left precental gyrus	10.21 ± 1.02	8.76 ± 0.72	4.43	0.00014
	Left inferior frontal gyrus (opercular part)	12.81 ± 1.17	11.24 ± 1.11	3.70	0.00098
	Right supplementary motor area	11.39 ± 0.74	10.12 ± 0.92	4.10	0.00034
	Left postcentral gyrus	10.26 ± 0.77	9.10 ± 0.78	4.04	0.0004
	Left precuneus	9.77 ± 0.91	8.25 ± 0.95	4.41	0.00015
	Left paracentral lobule	11.12 ± 0.84	9.65 ± 0.82	4.74	0.000061
	Right paracentral lobule	12.46 ± 1.10	10.70 ± 0.82	4.89	0.00004
CP1>CP2	Right putamen	12.12 ± 1.18	10.61 ± 0.75	4.05	0.00041
	Right thalamus	11.13 ± 1.68	9.21 ± 0.65	3.99	0.00048

CP1, children with bilateral spastic cerebral palsy before treatment; CP2, children with bilateral spastic cerebral palsy following treatment; HC, health children. FDR-corrected $P < 0.05$ indicated statistically significant differences between groups.

connectivity within the prefrontal basal ganglia circuits in the brain of BSCP.

Functional MRI study found that children with spastic diplegic CP had decreased regional homogeneity (ReHo) in the bilateral inferior frontal gyrus when compared with HC (42). Abnormal neural activity within the inferior frontal gyrus during the motor planning stage was also identified in children with CP, which was considered to be associated with tasks that required sustained vigilance (43, 44). The inferior frontal gyrus was also found to be involved in the process of executive planning and was necessary for matching the prescribed target forces (45). Based on these findings, it was possible that the impaired nodal parameters in the inferior frontal gyrus might indicate that children with BSCP had greater difficulty in sustaining their attention on the motor task demands.

Moreover, previous study with the network-based statistic (NBS) analysis demonstrated that fractional anisotropy (FA) with basal ganglia (mainly putamen and pallidum) and thalamus were significantly reduced in CP children (40). Gray matter lesions were also found in the basal ganglia of CP children, mainly located in bilateral putamen (46). The damaged posterior thalamic radiation connecting the thalamus to the posterior parietal and occipital cortex, was found to be associated with motor dysfunction in children with spastic CP (47). The motor network of CP was composed of the prefrontal, parietal regions, basal ganglia and thalamus (37), which were the most commonly affected subcortical structures in CP (40). The thalamus is the information integration center in the brain and is in the cortical-striatum-thalamus pathway (48). Therefore, impaired nodal metrics of basal ganglia and thalamus might be indirectly modulated by the stimulation of the cortical areas (49). The treatment of rTMS could modulate brain structural networks in children with BSCP and the modulated brain regions were associated with the improved motor and cognitive symptoms.

Several limitations should be noted in the present study. First, this was a small sample study and further studies with larger samples of children with CP were needed to advance the ability to generalize treatment outcomes of rTMS based on the method of MRI. Secondly, previous neuroimaging studies had identified aberrant functional connectivity in the brain of children with CP, therefore, future studies should employ structural-functional consistency analyses to fully elucidate the pathogenesis of CP. Thirdly, it was difficult to estimate the potential contribution of medication in relation to our results.

CONCLUSION

In conclusion, the present study revealed impaired topological organization in the prefrontal, parietal, occipital cortex and some subcortical regions in BSCP children. On the other hand, the results showed significant improvement of motor and cognitive function and changes of nodal parameters in the prefontal-striatum-thalamus of BSCP children in response to the rTMS treatment. All these findings suggested that rTMS might improve clinical

symptoms by modulating structural connectivity connecting to the prefontal-striatum-thalamus pathway for patients with BSCP.

DATA AVAILABILITY STATEMENT

The raw data supporting the conclusions of this article will be made available by the authors, without undue reservation.

ETHICS STATEMENT

The studies involving human participants were reviewed and approved by the Ethics Committee of the Children's Hospital of Nanjing Medical University. Written informed consent to participate in this study was provided by the participants' legal guardian/next of kin.

AUTHOR CONTRIBUTIONS

LZ, HX, JT, and XZ designed the experiments. MZ, YW, YL, WZ, and SZ contributed to clinical data collection and assessment. LZ and HX analyzed the results. LZ, HX, WZ, and SZ wrote the manuscript. JT and XZ approved the final manuscript. All authors contributed to the article and approved the submitted version.

FUNDING

The work was supported by the grants of: National Natural Science Foundation of China (Nos. 81501946 and 81401864); Science and Technology Development Fund of Nanjing Medical University (Nos. NJMUB2019183 and NJMUB2019188); Project of Jiangsu Maternal and Child Health Association (No. FYX201907).

REFERENCES

1. Van Naarden Braun K, Doernberg N, Schieve L, Christensen D, Goodman A, Yeargin-Allsopp M. Birth prevalence of cerebral palsy: a population-based study. *Pediatrics.* (2016) 137:1–9. doi: 10.1542/peds.2015-2872
2. Sellier E, Platt MJ, Andersen GL, I Krägeloh-Mann, De La Cruz J, Cans C. Decreasing prevalence in cerebral palsy: a multi-site European population-based study, 1980 to 2003. *Dev Med Child Neurol.* (2016) 58:85–92. doi: 10.1111/dmcn.12865
3. Gómez-Pérez C, JM Font-Llagunes, Martori JC, Vidal Samsó J. Gait parameters in children with bilateral spastic cerebral palsy: a systematic review of randomized controlled trials. *Dev Med Child Neurol.* (2019) 61:770–82. doi: 10.1111/dmcn.14108
4. Noble JJ, Gough M, Shortland AP. Selective motor control and gross motor function in bilateral spastic cerebral palsy. *Dev Med Child Neurol.* (2019) 61:57–61. doi: 10.1111/dmcn.14024
5. Papadelis C, Kaye H, Shore B, Snyder B, Grant PE, Rotenberg A. Maturation of corticospinal tracts in children with hemiplegic cerebral palsy assessed by diffusion tensor imaging and transcranial magnetic stimulation. *Front Hum Neurosci.* (2019) 13:254. doi: 10.3389/fnhum.2019.00254
6. Tekgul H, Saz U, Yilmaz S, Polat M, Aktan G, Kose T, et al. A transcranial magnetic stimulation study for the investigation of corticospinal motor pathways in children with cerebral palsy. *J Clin Neurosci.* (2020) 78:153–58. doi: 10.1016/j.jocn.2020.04.087
7. Galli J, Ambrosi C, Micheletti S, Merabet LB, Pinardi C, Gasparotti R, et al. White matter changes associated with cognitive visual dysfunctions in children with cerebral palsy: a diffusion tensor imaging study. *J Neurosci Res.* (2018) 96:1766–74. doi: 10.1002/jnr.24307
8. Kuo HC, Ferre CL, Carmel JB, Gowatsky JL, Stanford AD, Rowny SB, et al. Using diffusion tensor imaging to identify corticospinal tract projection patterns in children with unilateral spastic cerebral palsy. *Dev Med Child Neurol.* (2017) 59:65–71. doi: 10.1111/dmcn.13192
9. Mourão LF, Friel KM, Sheppard JJ, Kuo HC, Luchesi KF, Gordon AM, et al. The role of the corpus callosum in pediatric dysphagia: preliminary findings from a diffusion tensor imaging study in children with unilateral spastic cerebral palsy. *Dysphagia.* (2017) 32:703–13. doi: 10.1007/s00455-017-9816-0
10. Atkinson-Clement C, Pinto S, Eusebio A, Coulon O. Diffusion tensor imaging in Parkinson's disease: review and meta-analysis. *Neuroimage Clin.* (2017) 16:98–110. doi: 10.1016/j.nicl.2017.07.011
11. Puig J, Blasco G, Schlaug G, Stinear CM, Daunis-I-Estadella P, Biarnes C, et al. Diffusion tensor imaging as a prognostic biomarker for motor recovery and rehabilitation after stroke. *Neuroradiology.* (2017) 59:343–51. doi: 10.1007/s00234-017-1816-0
12. Tae WS, Ham BJ, Pyun SB, Kang SH, Kim BJ. Current clinical applications of diffusion-tensor imaging in neurological disorders. *J Clin Neurol.* (2018) 14:129–40. doi: 10.3988/jcn.2018.14.2.129
13. Van't Hooft J, van der Lee JH, Opmeer BC, Aarnoudse-Moens CS, Leenders AG, Mol BW, et al. Predicting developmental outcomes in premature infants by term equivalent MRI: systematic review and meta-analysis. *Syst Rev.* (2015) 4:71. doi: 10.1186/s13643-015-0058-7
14. Jiang H, Li X, Jin C, Wang M, Liu C, Chan KC, et al. Early diagnosis of spastic cerebral palsy in infants with periventricular white matter injury using diffusion tensor imaging. *AJNR Am J Neuroradiol.* (2019) 40:162–8. doi: 10.3174/ajnr.A5914
15. Condliffe EG, Jeffery DT, Emery DJ, Treit S, Beaulieu C, Gorassini MA. Full activation profiles and integrity of corticospinal pathways in adults with bilateral spastic cerebral palsy. *Neurorehabil Neural Repair.* (2019) 33:59–69. doi: 10.1177/1545968318818898
16. Carneiro MIS, Russo C, Masson R, Sebastiano DR, Baranello G, Turati C, et al. Motor learning in unilateral cerebral palsy and the influence of corticospinal tract reorganization. *Eur J Paediatr Neurol.* (2020) 27:49–59. doi: 10.1016/j.ejpn.2020.04.013
17. Aravamuthan BR, Waugh JL. Localization of basal ganglia and thalamic damage in dyskinetic cerebral palsy. *Pediatr Neurol.* (2016) 54:11–21. doi: 10.1016/j.pediatrneurol.2015.10.005
18. Krägeloh-Mann I. Grey matter injury in cerebral palsy - pallidum for the role of the predicting severity. *Dev Med Child Neurol.* (2015) 57:1089–90. doi: 10.1111/dmcn.12822
19. Jiang H, Liu H, Huang T, Wu L, Wu F, Liu C, et al. Structural network performance for early diagnosis of spastic cerebral palsy in periventricular white matter injury. *Brain Imaging Behav.* (2020). doi: 10.1007/s11682-020-00295-6. [Epub ahead of print].
20. Ceschin R, Lee VK, Schmithorst V, Panigrahy A. Regional vulnerability of longitudinal cortical association connectivity: associated with structural network topology alterations in preterm children with cerebral palsy. *Neuroimage Clin.* (2015) 9:322–37. doi: 10.1016/j.nicl.2015.08.021
21. Englander ZA, Pizoli CE, Batrachenko A, Sun J, Worley G, Mikati MA, et al. Diffuse reduction of white matter connectivity in cerebral palsy with specific vulnerability of long range fiber tracts. *Neuroimage Clin.* (2013) 2:440–7. doi: 10.1016/j.nicl.2013.03.006
22. Palisano RJ, Avery L, Gorter JW, Galuppi B, McCoy SW. Stability of the gross motor function classification system, manual ability classification system, and communication function classification system. *Dev Med Child Neurol.* (2018) 60:1026–32. doi: 10.1111/dmcn.13903
23. Yang J, Hu L, Zhang Y, Shi Y, Jiang W, Song C. Gesell developmental schedules scores and the relevant factors in children with down syndrome. *J Pediatr Endocrinol Metab.* (2020) 33:539–46. doi: 10.1515/jpem-2019-0236

24. Tan T, Wang W, Xu H, Huang Z, Wang YT, Dong Z. Low-Frequency rTMS ameliorates autistic-like behaviors in rats induced by neonatal isolation through regulating the synaptic GABA transmission. *Front Cell Neurosci.* (2018) 12:46. doi: 10.3389/fncel.2018.00046
25. Gordon PC, Zrenner C, Desideri D, Belardinelli P, Zrenner B, Brunoni AR, et al. Modulation of cortical responses by transcranial direct current stimulation of dorsolateral prefrontal cortex: a resting-state EEG and TMS-EEG study. *Brain Stimul.* (2018) 11:1024–32. doi: 10.1016/j.brs.2018.06.004
26. Rogasch NC, Daskalakis ZJ, Fitzgerald PB. Cortical inhibition of distinct mechanisms in the dorsolateral prefrontal cortex is related to working memory performance: a TMS-EEG study. *Cortex.* (2015) 64:68–77. doi: 10.1016/j.cortex.2014.10.003
27. Zhang C, Zheng X, Lu R, Yun W, Yun H, Zhou X. Repetitive transcranial magnetic stimulation in combination with neuromuscular electrical stimulation for treatment of post-stroke dysphagia. *J Int Med Res.* (2019) 47:662–72. doi: 10.1177/0300060518807340
28. Smith SM, Jenkinson M, Woolrich MW, Beckmann CF, Behrens TE, Johansen-Berg H, et al. Advances in functional structural MR image analysis implementation as FSL. *Neuroimage.* (2004) 23(Suppl. 1):S208–19. doi: 10.1016/j.neuroimage.2004.07.051
29. Tzourio-Mazoyer N, Landeau B, Papathanassiou D, Crivello F, Etard O, Delcroix N, et al. Automated anatomical labeling of activations in SPM using a macroscopic anatomical parcellation of the MNI MRI single-subject brain. *Neuroimage.* (2002) 15:273–89. doi: 10.1006/nimg.2001.0978
30. Rubinov M, Sporns O. Complex network measures of brain connectivity: uses and interpretations. *Neuroimage.* (2010) 52:1059–69. doi: 10.1016/j.neuroimage.2009.10.003
31. Shang Q, Ma CY, Lv N, Lv ZL, Yan YB, Wu ZR, et al. Clinical study of cerebral palsy in 408 children with periventricular leukomalacia. *Exp Ther Med.* (2015) 9:1336–44. doi: 10.3892/etm.2015.2222
32. Cho HK, Jang SH, Lee E, Kim SY, Kim S, Kwon YH, et al. Diffusion tensor imaging-demonstrated differences between hemiplegic and diplegic cerebral palsy with symmetric periventricular leukomalacia. *AJNR Am J Neuroradiol.* (2013) 34:650–4. doi: 10.3174/ajnr.A3272
33. Hamer EG, Vermeulen RJ, Dijkstra LJ, Hielkema T, Kos C, Bos AF, et al. Slow pupillary light responses in infants at high risk of cerebral palsy were associated with periventricular leukomalacia and neurological outcome. *Acta Paediatr.* (2016) 105:1493–501. doi: 10.1111/apa.13532
34. Parikh NA, Hershey A, Altaye M. Early detection of cerebral palsy using sensorimotor tract biomarkers in very preterm infants. *Pediatr Neurol.* (2019) 98:53–60. doi: 10.1016/j.pediatrneurol.2019.05.001
35. de Almeida Carvalho Duarte N, Collange Grecco LA, Zanon N, Galli M, Fregni F, Santos Oliveira C. Motor cortex plasticity in children with spastic cerebral palsy: a systematic review. *J Mot Behav.* (2017) 49:355–64. doi: 10.1080/00222895.2016.1219310
36. Surkar SM, Hoffman RM, Willett S, Flegle J, Harbourne R, Kurz MJ. Hand-arm bimanual intensive therapy improves prefrontal cortex activation in children with hemiplegic cerebral palsy. *Pediatr Phys Ther.* (2018) 30:93–100. doi: 10.1097/PEP.0000000000000486
37. Lee D, Pae C, Lee JD, Park ES, Cho SR, Um MH, et al. Analysis of structure-function network decoupling in the brain systems of spastic diplegic cerebral palsy. *Hum Brain Mapp.* (2017) 38:5292–306. doi: 10.1002/hbm.23738
38. Weierink L, Vermeulen RJ, Boyd RN. Brain structure and executive functions in children with cerebral palsy: a systematic review. *Res Dev Disabil.* (2013) 34:1678–88. doi: 10.1016/j.ridd.2013.01.035
39. Reid SM, Dagia CD, Ditchfield MR, Reddihough DS. Grey matter injury patterns in cerebral palsy: associations between structural involvement on MRI and clinical outcomes. *Dev Med Child Neurol.* (2015) 57:1159–67. doi: 10.1111/dmcn.12800
40. Ballester-Plané J, Schmidt R, Laporta-Hoyos O, Junqué C, Vázquez É, Delgado I, et al. Whole-brain structural connectivity in dyskinetic cerebral palsy and its association with motor and cognitive function. *Hum Brain Mapp.* (2017) 38:4594–612. doi: 10.1002/hbm.23686
41. Burke MJ, Fried PJ, Pascual-Leone A. Transcranial magnetic stimulation: neurophysiological and clinical applications. *Handb Clin Neurol.* (2019) 163:73–92. doi: 10.1016/B978-0-12-804281-6.00005-7
42. Mu X, Wang Z, Nie B, Duan S, Ma Q, Dai G, et al. Altered regional and circuit resting-state activity in patients with occult spastic diplegic cerebral palsy. *Pediatr Neonatol.* (2018) 59:345–51. doi: 10.1016/j.pedneo.2017.10.003
43. Kurz MJ, Proskovec AL, Gehringer JE, Heinrichs-Graham E, Wilson TW. Children with cerebral palsy have altered oscillatory activity in the motor and visual cortices during a knee motor task. *Neuroimage Clin.* (2017) 15:298–305. doi: 10.1016/j.nicl.2017.05.008
44. Kim JH, Kim DW, Im CH. Brain areas responsible for vigilance: an EEG source imaging study. *Brain Topogr.* (2017) 30:343–51. doi: 10.1007/s10548-016-0540-0
45. Wiers CE, Gawron CK, Gröpper S, Spengler S, Stuke H, Lindenmeyer J, et al. Decreased gray matter volume in inferior frontal gyrus is related to stop-signal task performance in alcohol-dependent patients. *Psychiatr Res.* (2015) 233:125–30. doi: 10.1016/j.pscychresns.2015.05.006
46. Qin Y, Sun B, Zhang H, Li Y, Zhang T, Luo C, et al. Aberrant interhemispheric functional organization in children with dyskinetic cerebral palsy. *Biomed Res Int.* (2019) 2019:4362539. doi: 10.1155/2019/4362539
47. Hoon AH, Jr., Stashinko EE, Nagae LM, Lin DD, Keller J, Bastian A, et al. Sensory and motor deficits in children with cerebral palsy born preterm correlate with diffusion tensor imaging abnormalities in thalamocortical pathways. *Dev Med Child Neurol.* (2009) 51:697–704. doi: 10.1111/j.1469-8749.2009.03306.x
48. Tsubokawa T, Katayama Y, Yamamoto T, Hirayama T, Koyama S. Treatment of thalamic pain by chronic motor cortex stimulation. *Pacing Clin Electrophysiol.* (1991) 14:131–4. doi: 10.1111/j.1540-8159.1991.tb04058.x
49. Pei Q, Zhuo Z, Jing B, Meng Q, Ma X, Mo X, et al. The effects of repetitive transcranial magnetic stimulation on the whole-brain functional network of postherpetic neuralgia patients. *Medicine.* (2019) 98:e16105. doi: 10.1097/MD.0000000000016105

Conflict of Interest: The authors declare that the research was conducted in the absence of any commercial or financial relationships that could be construed as a potential conflict of interest.